International Journal of Mass Spectrometry and Ion Physics, 53 (1983) 227—242
Elsevier Science Publishers B.V., Amsterdam — Printed in The Netherlands

PROMPT AND METASTABLE DECOMPOSITIONS IN ^{252}Cf FISSION FRAGMENT IONIZATION MASS SPECTROMETRY*

B.T. CHAIT
The Rockefeller University, New York, New York 10021 (U.S.A.)

ABSTRACT

High energy ion bombardment of organic compounds in the condensed phase is found to give rise to secondary molecular ions in the gas phase containing appreciable internal energy of excitation. This paper presents the results of time-of-flight mass spectrometric studies of the subsequent prompt and metastable decomposition of these excited ions. The implications of the findings on the fragmentation mechanisms involved in heavy particle bombardment mass spectrometry is discussed.

INTRODUCTION

The bombardment of organic compounds in the condensed phase by 100 MeV heavy ions and ions and atoms with energies of a few to tens of keV all give rise to secondary ions in the gas phase containing appreciable internal energy of excitation (refs.1-5). We have made detailed studies of the subsequent prompt and metastable decomposition of these excited ions using the ^{252}Cf fission fragment induced ionization mass spectrometer at the Rockefeller University (refs.1,3,4). Although this is a time-of-flight instrument, our findings have rather general implications for practitioners of heavy particle bombardment techniques using conventional magnetic deflection and quadrupole mass spectrometers.

PROMPT AND METASTABLE FRAGMENTATION

Prompt fragmentations are normally associated with peaks in the mass spectrum that are sharp and appear at the expected mass for the fragment. Such sharp fragment peaks will arise from decompositions occurring prior to the precurser ion attaining significant kinetic energy or before it is extracted into the mass spectrometer. Metastable fragmentations, on the other hand, are usually associated with peaks that may be broad, exhibit tails and/or appear at masses not normally expected for the fragments. It is clear, however, that this way

*Dedicated to Professor R.D. Macfarlane on the occassion of his 50th birthday and presented at a symposium held in his honor at College Station, Tx. USA 15-18 May 1983.

0020-7381/83/$03.00

of defining metastable and prompt fragmentation is very dependent on the mass spectrometer and the experimental conditions utilized. This point is illustrated in Table 1 where the decomposition of a mass 1000 ion is considered in three different classes of mass spectrometer.

TABLE 1

Typical prompt and metastable decomposition times after ion formation in three different classes of mass spectrometer

INSTRUMENT	PROMPT DECOMPOSITIONS (s)	METASTABLE DECOMPOSITIONS (s)
Time-of-flight	$\lesssim 10^{-8} - 10^{-9}$	$10^{-8} - 10^{-4}$
Magnetic Deflection	$\lesssim 10^{-6} - 5\times10^{-6}$	$10^{-6} - 5\times10^{-5}$
Quadrupole	$\lesssim 2\times10^{-6} - 2\times10^{-5}$	Not generally detected

For the time-of-flight mass spectrometer with a typical extraction field of 30000-50000 V/cm (refs.6,2,4) prompt decompositions leading to sharp peaks occur in times $\lesssim 10^{-8} - 10^{-9}$ s after ion formation while metastable decompositions may be continuously detected in times ranging from $10^{-8} - 10^{-4}$ s. For magnetic and quadrupole instruments, it is most usual to extract the ions from the sample holder with a low field (some tens of V/cm) so that prompt decompositions would in these cases be those occurring in $10^{-6} - 10^{-5}$ s after ion formation. For magnetic deflection instruments metastable decompositions are usually detected in the time range $10^{-6} - 5\times10^{-5}$ s in selected regions of the mass spectrometer.

FRAGMENTATION IN HEAVY PARTICLE BOMBARDMENT MASS SPECTROMETRY

Some general features of energetic heavy ion bombardment mass spectra are illustrated in Figs. 1 and 2. Some molecular ion species undergo very little fragmentation like that from the cationic dye molecule crystal violet (see Fig. 1) where the quasi-molecular ion at m/z 372 retains 75% of the total ionization. More usually, however, very extensive fragmentation of the molecular ion is observed as in the 31 amino acid residue neuropeptide β-Endorphin (see Fig. 2) where the quasi-molecular ions at mass ~3500 retain only .01% of the total ionization. The tremendous analytical utility of these heavy particle impact methods resides in the fact that, even for very large involatile molecules, frequently enough quasi-molecular ions survive fragmentation to define the molecular weight of the compound (refs.7,8).

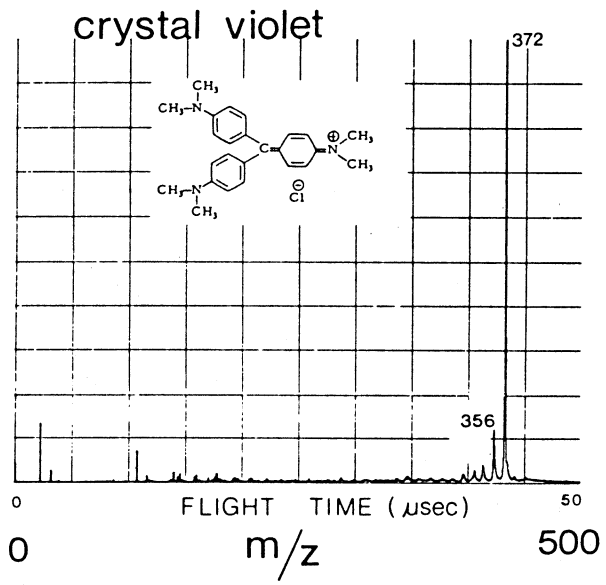

Fig. 1. ^{252}Cf time-of-flight mass spectrum of crystal violet. Positive ions.

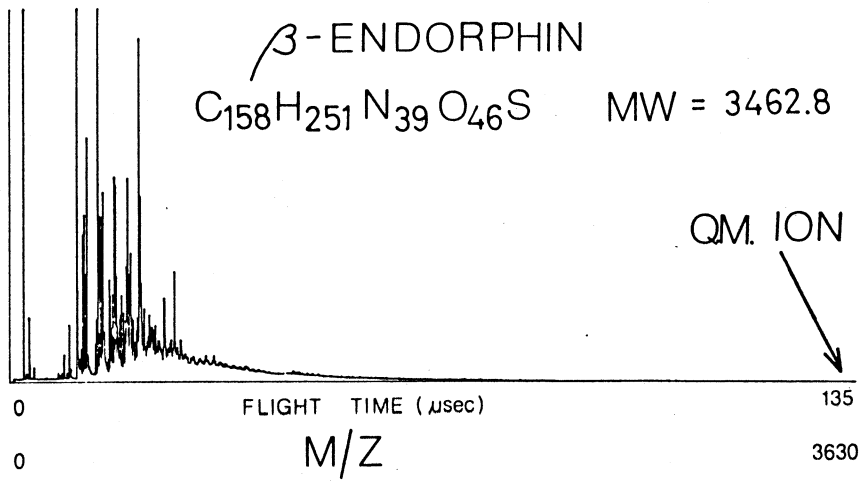

Fig. 2. ^{252}Cf time-of-flight mass spectrum of β-Endorphin. Positive ions.

	$(M+H)^+$	$(M+Na)^+$	$(M+K)^+$
MEASURED MASS	3465.2	3486.9	3503.3
CALCULATED MASS	3465.7	3487.7	3503.7
MASS DIFFERENCE (amu)	-0.5	-0.8	-0.4

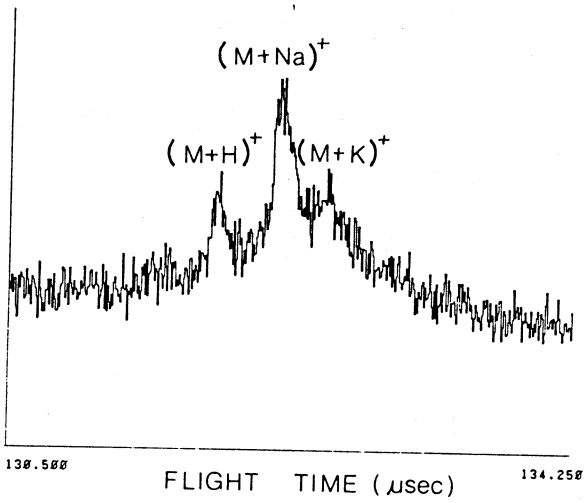

Fig. 3. Detail of the molecular region of the positive time-of-flight spectrum of β-Endorphin.

Fig. 3 shows a detail of the molecular ion region of β-Endorphin, blown up by a factor of 3000 in intensity with respect to Fig. 2. Peaks corresponding to protonated, sodium cationized and potassium cationized molecular ions are observed with the measured isotopically averaged molecular weights in good agreement with the isotopically averaged molecular weights calculated for β-Endorphin. The large amounts of fragmentation observed (see also refs.4 and 3) implies that most of the molecular ions formed with ^{252}Cf fission fragments (and also with keV ions and atoms (refs.2,9,5)) are produced with considerable internal energy of excitation. What follows is a brief overview of our investigations of the metastable decomposition of these excited species using the ^{252}Cf fission fragment time-of-flight mass spectrometer at the Rockefeller University shown schematically in Fig. 4.

EXPERIMENTAL INVESTIGATIONS OF METASTABLE DECOMPOSITIONS

Fragmentation Kinetics

As a specific example we shall consider the detailed fate of a molecule of chlorophyll *a* (Chl *a*) (see Fig. 5) initially bound at the surface of the sample foil upon bombardment by a fission fragment. The fission fragment passes through and deposits energy in a 1000A° thick layer of Chl *a* in the order of 10^{-14} s. Through processes that are not presently understood in detail, the passage of the heavy ion causes the Chl *a* molecule to be ejected from the surface and ionized. There is evidence (refs.10,11) to suggest that the molecular

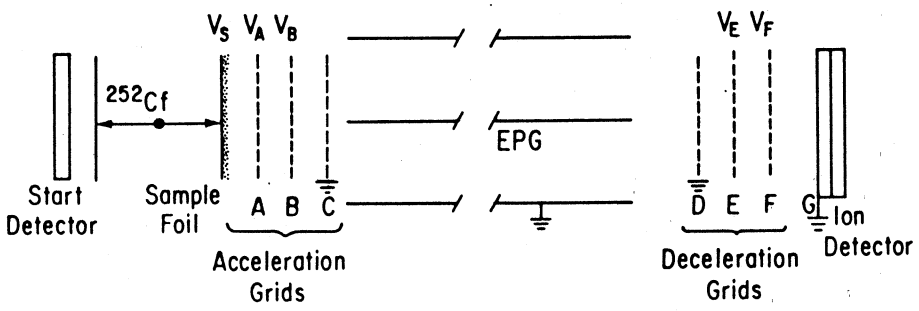

Fig. 4 Fission fragment ionization MS. EPG is the electrostatic particle guide, which enhances transport of ions down the 3m flight tube.

ions acquire a distribution of energies less than or of the order of a few eV during the ejection process. We assume, for the purpose of illustration that the ejected ion acquires leV in the initial desorption process. After 10^{-14} s the molecular ion, if it has formed, still exists on the surface. If it is then accelerated without fragmenting it will acquire the full acceleration energy and drift down the flight tube to the detector. Such ions will produce a sharp molecular ion peak in the time-of-flight spectrum as indicated in Fig. 6 with a line-width in our instrument corresponding to a resolution of 2000 FWHM. This line-width which corresponds to 17 ns for a flight time of 67.5 μs for the molecular ion at m/z 892 arises both from the initial distribution of kinetic energies of the secondary ions and from purely instrumental effects like non-uniform accelerating fields. If it breaks up promptly on the surface, the fragment will have a lower mass and hence a shorter flight time and produce a sharp peak as indicated in Fig. 6. The specific fragmentation reaction under consideration is $M^{\cdot +} \longrightarrow 614^{\cdot +} + 278°$ i.e. the elimination of

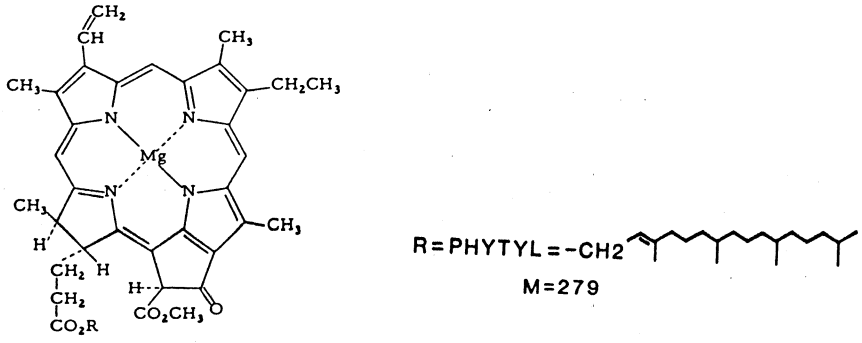

Fig. 5. Structure of chlorophyll a.

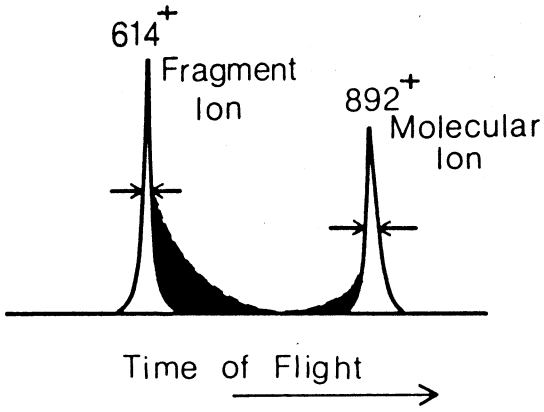

Fig. 6. Time-of-flight spectrum showing the effect of fragmentations occurring during ion acceleration.

the phytyl hydrocarbon tail from the Chl a molecular ion. Columns 2 and 3 of Table 2 give calculated values, as a function of time, of the distance travelled and the energy acquired by the molecular ion at the point of breakup. Upon fragmentation the energy acquired by the precurser ion partitions into the ion fragment and the neutral fragment. The energy taken away by the neutral (31%) is lost to the ion fragment and so fragment ions thus formed will have energies lower than those fragments which acquire the full acceleration potential. The 4th column of Table 2 indicates the resulting delay with respect to the centroid of the prompt fragmentation peak in the time-of-flight spectrum. For times between 10^{-14} and 10^{-9} s, the molecular ion is seen to move primarily under the influence of the initial kinetic energy acquired during ejection. At later times significant energies are acquired from the accelerating field resulting in progressively longer flight time delays of such fragment ions with respect to prompt fragments. The sum total of these breakups during acceleration gives rise to the shaded continuum (see Fig. 6) stretching between the precurser and fragment ion peaks. Actual time-of-flight data showing fragmentation in the acceleration region for the transition described above is given in Fig. 7. Several points are marked on the curve indicating the time of fragmentation after molecular ion formation. It is observed that fragmentations in times between 10^{-14} and 10^{-9} s all contribute just to the sharp fragment peak. Thus we can say nothing in detail about the distribution of rate constants for disintegrations at these earlier times. The tail shows fragmentations occurring across the whole acceleration region giving detailed information about the distributions of fragmentations at times between 10^{-8} - 10^{-7} s.

TABLE
Calcul
to pro

Time o fragme after format (s)
10^{-14}
10^{-13}
10^{-12}
10^{-11}
10^{-10}
10^{-9}
10^{-8}
10^{-7}

Fig. 7.
fragmen

TABLE 2.

Calculations of the flight-time differences of delayed fragments with respect to prompt fragments in an accelerating field of 30000 V/cm

Time of fragmentation after ion formation (s)	Distance travelled by molecular ion (A°)	Energy Acquired by molecular ion (eV)	Time-of-flight delay of delayed fragment with respect to prompt fragment (ns)
10^{-14}	0	1.0	0.0
10^{-13}	4.7×10^{-1}	1.0	0.0
10^{-12}	4.7×10^{0}	1.0	0.0
10^{-11}	4.7×10^{1}	1.0	0.0
10^{-10}	4.8×10^{2}	1.1	0.1
10^{-9}	6.3×10^{3}	2.9	1.7
10^{-8}	2.1×10^{5}	64	55
10^{-7}	1.7×10^{7}	5011	4572

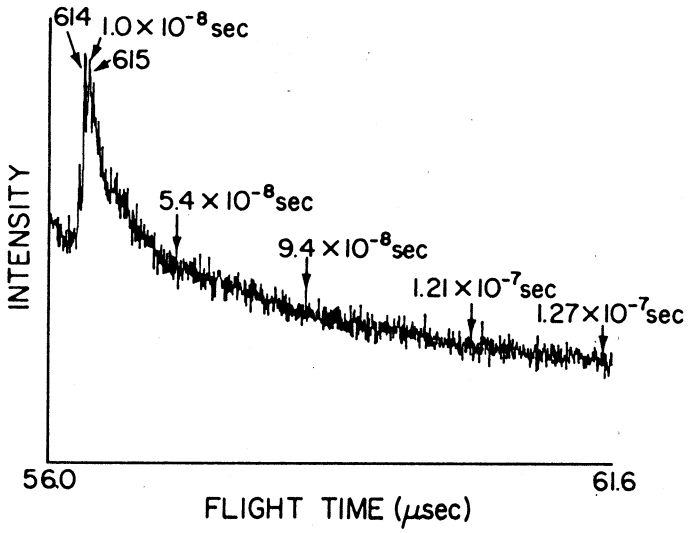

Fig. 7. High time tail on the m/z 614 peak resulting from the delayed fragmentation reaction $_{M}{}^{\cdot+} \longrightarrow 614^{\cdot+} + 278$ of Chl a.

Thus we see that such time-of-flight studies where the extraction field is 30,000 V/cm gives fragmentation kinetics information down to times two orders of magnitude earlier than that usually obtained with fast atom bombardment on deflection instruments. This is still three orders of magnitude later in time than the kinetics information obtainable with the very large non-uniform fields used in field ionization and field desorption (ref.12). We have also investigated the fragmentation kinetics at later times. Between 175 and 285 ns after parent ion formation, the mean lifetime of molecular ions was determined to be 227 ns. If all the molecular ions have a lifetime of only 227 ns, essentially none would survive the 67.5 μs flight to the detector. In fact, a fraction do survive, implying that at least some have a significantly longer lifetime ($>10^{-5}$ s). In summary, we observe prompt fragmentations for times less than 10^{-8} s as well as much fragmentation in times between 10^{-8} and a few times 10^{-5} s, i.e. disintegrations exhibiting a wide range of rate constants.

Metastable Decompositions in the Field-Free Flight Tube

The bottom panel of Fig. 8 shows an ion with mass M, energy E and velocity V fragmenting in the field-free flight tube. If no internal energy of excitation is released in the form of translational energy of the fragments during the decomposition, the flight times of the metastable fragments with mass m_f and m_o will be the same as the precurser ion, since their velocieities are unchanged. Thus the parent ion as well as the metastable daughter ion and neutral will all contribute to a single peak in the spectrum if the fragmentation takes place in the field-free flight-tube. The consequence of this is that fragmentations taking place between 10^{-7} and 10^{-4} s are not lost to the spectrum at all in this instrument, in contrast to the situation with deflection and quadrupole mass spectrometers. Thus the normal time-of-flight spectrum is indicative of the distribution of molecular and fragment ions after a time of about 100 ns after ion formation in contrast to a deflection or quadrupole MS which largely represents ions which survive for perhaps 30-150 μs.

Normally, internal energy of excitation is released as kinetic energy during the fragmentation. The fragments will thus acquire a spread of velocities about the mean velocity V which shows up as a broadening of the time-of-flight peak. This has the major consequence that heavy particle bombardment time-of-flight mass spectra have a completely different look to conventional mass spectra, exhibiting very broad peaks and extensive continuua. An example is given in the lower panel of Fig. 8 showing the protonated molecular ion peak of the nucleoside guanosine at m/z 284. The hatched broad component of the peak arises from the fragmentation reaction

$$(M+H)^+ \longrightarrow \underset{m/z\ 152}{(\text{base} + 2H)^+} + \text{neutral}$$

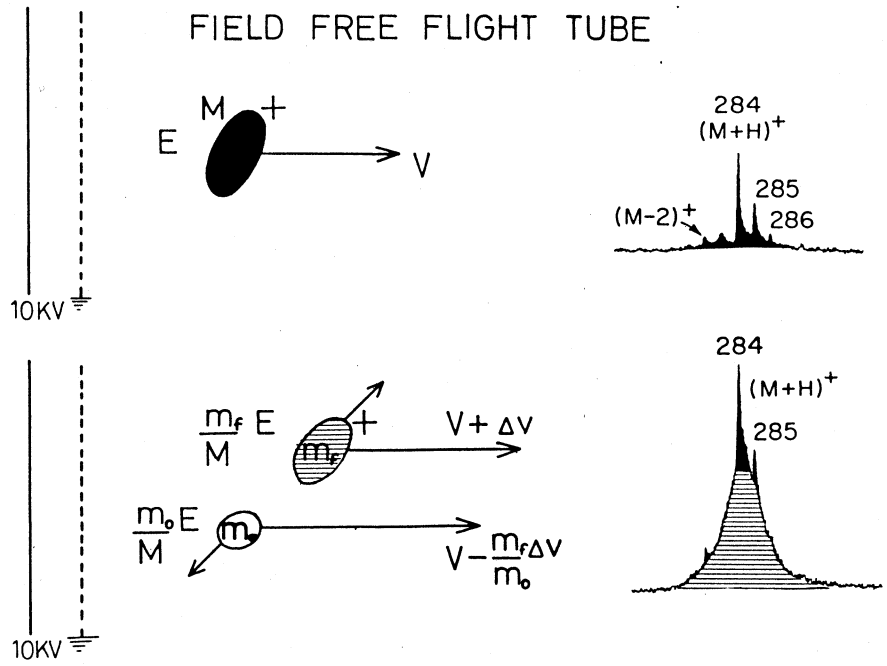

Fig. 8. Metastable fragmentation in the field-free flight-tube. Bottom panel shows protonated guanosine molecular ion peak containing both metastable fragment and stable ion components. Top panel shows protonated guanosine molecular ion peak containing only stable ion component.

in the flight tube with the release of internal energy. The sharp component of the peak indicated in black arises from protonated molecular ions which do not fragment in flight. As shown in Fig. 8, the energies of the fragments are lower than the precurser ion. It is thus possible to reject the fragments altogether by applying the appropriate potentials to the deceleration grids (see Fig. 4), resulting in the resolution enhanced peaks shown in the top panel of Fig. 8. Shown in Fig. 9 is part of the positive ion spectrum of Chl *a* between masses 400-1000 taken under 2 different conditions. The top panel shows the spectrum taken with no deceleration potential while the bottom panel shows the spectrum taken with a deceleration potential equal to 99% of the acceleration potential. Thus all flight tube decomposition products with masses less than 99% that of their precurser ions are rejected. Fully 78% of the ions

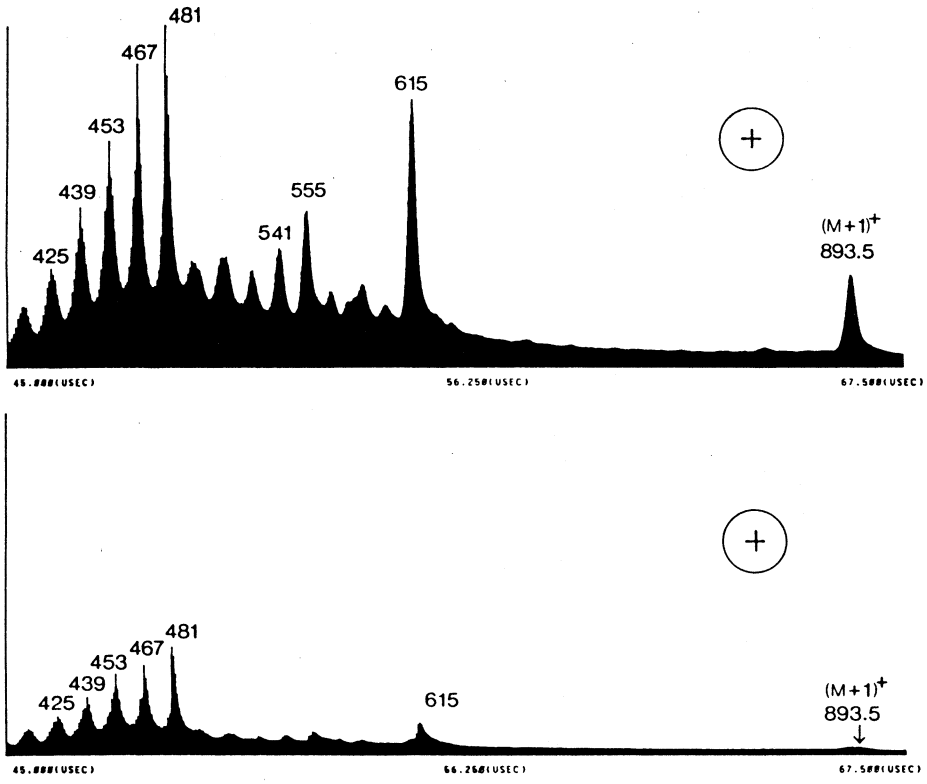

Fig. 9. Positive spectra of Chl a between m/z 400-1000. Top panel - spectrum taken with deceleration potential = 0. Bottom panel - spectrum taken with deceleration potential = 99% of acceleration potential.

entering the flight tube fragment in it in transit to the detector, i.e., only 22% do not fragment in times between 10^{-7} and 10^{-4} s. In particular only 1.1% of the molecular ions survive the flight, 8.5% of the ions in the mass range 611-618, 8.3% in the range 486-610 and 36% in the range 411-485. To recapitulate, the top spectrum corresponds to the distribution of ions after approximately 100 ns while the bottom corresponds to the distribution of ions after 45-67 μs, a time closer to that pertaining to observations in deflection and quadrupole instruments.

We, however, do not have to reject the metastable fragments altogether. Rather by applying the appropriate potentials to the deceleration grids it is possible (ref.1) to separate the fragment ions from their precurser ions as indicated in Fig. 10 which gives the molecular ion region of a Chl a sample containing a small amount of pheophytin a (Pheo a = Chl a - Mg + 2H). By measuring the time separation Δt between the broad metastable peak and its sharp precurser peak we can determine the mass of the metastable daughter ion

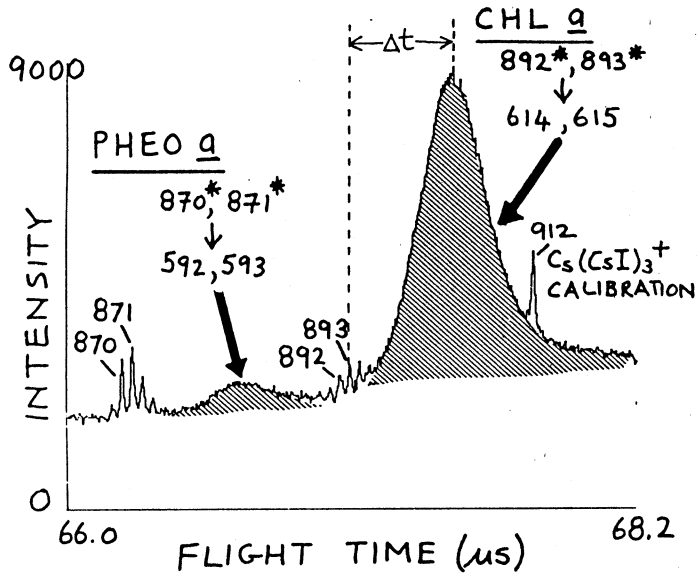

Fig. 10. Separation of peaks from flight tube fragmentation ions (cross-hatched) and sharp peaks from ions not fragmenting in the flight tube.

(refs.13,14). The neutral loss from both Chl a and Pheo a was determined to be 279 ± 2 amu corresponding to the elimination of the phytyl hydrocarbon tail. In this way we have obtained maps of the majority of the intense metastable fragmentation in Chl a for both positive ions (see Fig. 11) and negative ions (see Fig. 12). Details of the metastable fragmentation reactions are described elsewhere (ref. 14) where we find that we can rationalize much of the fragmentation in a straightforward way.

FRAGMENTATION MECHANISMS

Our overall observations are compatible with the organic ions being formed in the initial volatilization ionization process with a distribution of excitation energies and these differing excitation energies will produce fragmentations proceeding at differing rates. Our findings lead us to suggest that the fission fragment induced fragmentation processes observed for these organic species involve many of the concepts embodied in the quasi-equilibrium theory (QET) of mass spectra. We consider now briefly the implications of the QET as applied to the very large molecules which are being examined by heavy particle bombardment mass spectrometry.

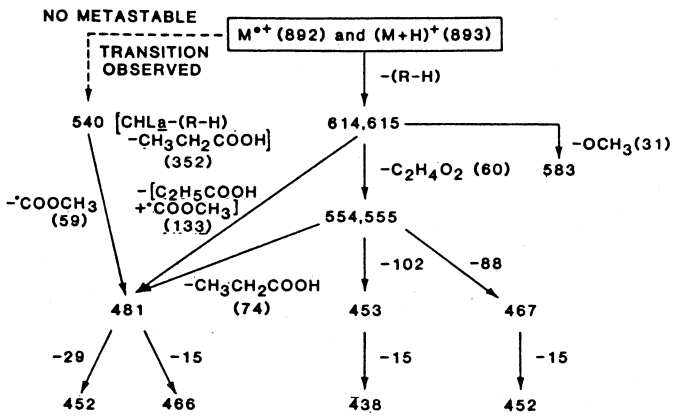

Fig. 11. Positive ion flight-tube metastable fragmentation scheme for Chl a.

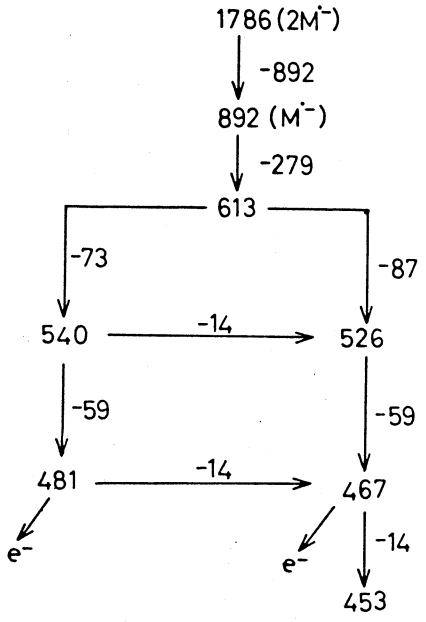

Fig 12. Negative ion flight-tube metastable fragmentation scheme for Chl a.

A simple classical rate expression for unimolecular fragmentation based on the harmonic oscillator model is given by (ref. 15)

$$K(E) = \nu \left(\frac{E-E_o}{E} \right)^{s-1} \qquad (1)$$

where

ν is the frequency factor
E the internal energy
E_o the activation energy
s the effective number of oscillators taken here to be simply 1/3 (3N-6)
N the number of atoms

We will use this simple expression to consider two cases:

1) a simple single bond cleavage reaction with a frequency factor of 4×10^{13} s^{-1} compatible with cleavage occurring in a single vibration of the bond and a high activation energy typical of a simple bond break, 3 eV.

2) a re-arrangement reaction with a much lower frequency factor of 3×10^{10} s^{-1} corresponding to the fact that these reactions are much less favored entropically, but with a low activation energy, 1 eV.

The curves shown in Fig. 13 are calculated rate constants based on the classical expression (1) as a function of energy for a molecule like Chl a with 137 atoms. The calculation predicts that for internal energies up to almost 40 eV the entropically unfavored re-arrangement reactions will dominate strongly over simple bond breaking reactions and only at very high energies do these bond breaking reactions begin to take over. Experimentally we observe that 4-centre elimination reactions and other low energy re-arrangement processes do indeed dominate the fission fragment spectra, at least for those portions of the spectra which we can understand in a straightforward way. Similarly with a molecule of the size of β-Endorphin with ~500 atoms we obtain the curves in Fig. 14. The trends are of course similar. Up to very high internal energies, approaching 140 eV, re-arrangement reactions dominate. Again this is in accord with experimental observations. It is observed that a molecule of this size can hold a great deal of energy, although the energy per degree of freedom is comparable with smaller molecules.

Inspection of the spectrum of β-Endorphin (Fig. 2) reveals that the spectrum is composed largely of low molecular weight fragments. This rather characteristic distribution, consisting of a quasi-molecular ion, then a sort of desert with the fragmentation increasing exponentially to lower masses, is frequently observed in fission fragment spectra. One may inquire as to the

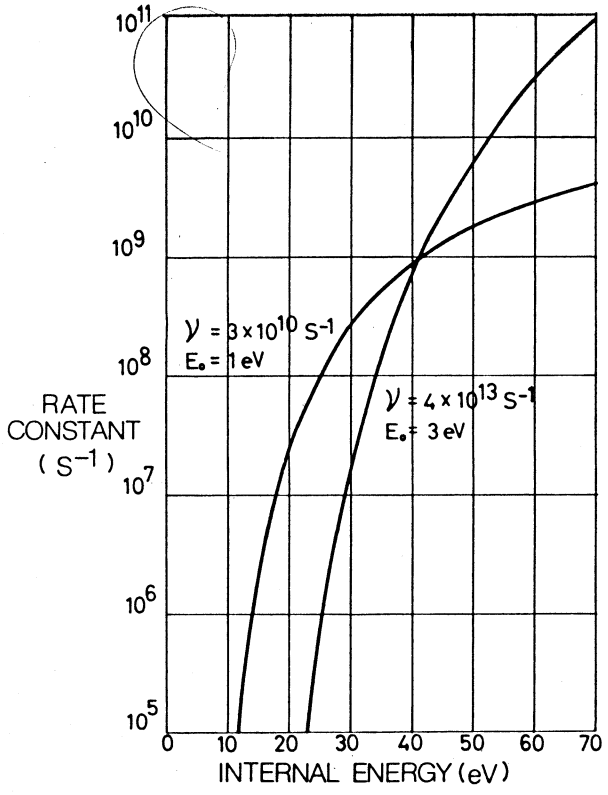

Fig. 13. Calculated rate constants as a function of internal energy using the expression (1) for a molecule containing 137 atoms.

origins of this distribution of ions. Certainly there are detailed chemical structural factors involved as well as straightforward probability considerations favoring lower mass fragments. However, examination of the curves in Fig. 14 suggest a further explanation. We see that a molecule of this size can hold a great deal of energy - many tens of eV before the probability for fragmentation becomes high. Also we see that low energy re-arrangements will dominate in this region and that a single low energy fragmentation takes away only a very small proportion of the total energy contained in the molecule. Table 3 gives the calculated rate constants for successive fragmentations of a molecule with a mass of 3500, where each fragmentation splits the remaining ion in half. The calculation assumes equipartition of energy - i.e., the fragment ion retains half of the total remaining energy of the precurser ion. The rate constant for fragmentation is calculated to decrease very slowly indeed, implying that if a reaction to break such a molecule in half proceeds with a rate constant of $10^9\ s^{-1}$, then subsequent successive fragmentation

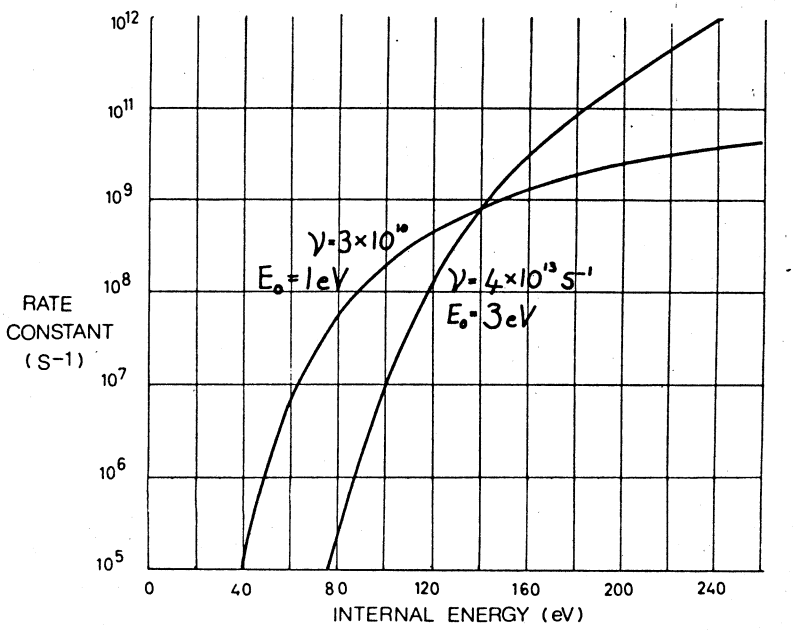

Fig. 14. Calculated rate constants as a function of internal energy using the expression (1) for a molecule containing 500 atoms.

TABLE 3

Rate constants for successive fragmentations. Activation energy for a fragmentation = 1 eV. Frequency factor = 3×10^{10} s^{-1}

MASS	ENERGY CONTENT (eV)	NO. OF DEGREES OF FREEDOM	RATE CONSTANT (s^{-1})
3500	140.0	500	8.3×10^{8}
1750	69.5	250	8.0×10^{8}
875	34.3	125	7.4×10^{8}
437	16.7	62	6.3×10^{8}
218	7.8	31	4.1×10^{8}

reactions are also highly probable, resulting in a predominance of low mass fragments. Our direct observation of sequential metastable reactions occurring with high probability for Chl a (see Figs. 11 and 12) provides further confirmation for these notions.

ACKNOWLEDGEMENTS

This work was supported by a grant from the Division of Research Resources, National Institutes of Health. I am grateful to Dr. F. H. Field for helpful discussion.

REFERENCES

1 B.T. Chait and F.H. Field, Int. J. Mass Spectrom. Ion Physics., 41 (1981) 17.
2 B.T. Chait and K.G. Standing, Int. J. Mass Spectrom. Ion Physics, 40 (1981) 185.
3 B.T. Chait and F.H. Field, J. Am. Chem. Soc. 104 (1982) 5519.
4 B.T. Chait, W.C. Agosta and F.H. Field, Int. J. Mass Spectrom. Ion Phys., 39 (1981) 339.
5 M. Barber, R.S. Bordoli, G.J. Elliott, R.D. Sedgwick and A.N. Tyler, Anal. Chem. 54 (1982) 645 A.
6 R.D. Macfarlane and D.F. Torgerson, Int. J. Mass Spectrom. Ion Phys., 21 (1976) 81.
7 R.D. Macfarlane and D.F. Torgerson, Science 191 (1976) 920.
8 B. Sundqvist, A. Hedin, P. Hakansson, I. Kamensky, J. Kjellberg, M. Salehpour G. Sawe and S. Widdiyasekera, Present Proceedings.
9 W. Ens, K.G. Standing, B.T. Chait and F.H. Field, Anal. Chem. 53 (1981) 1241.
10 P. Duck, W. Treu, W. Galster, H. Frohlich and H. Voit, Nucl. Instr. Meth. 168 (1980) 601
11 K. Wien, O. Becker, P. Daab and D. Nederveld, Nucl. Instr. Meth. 170 (1980) 601.
12 H.D. Beckey, Principles of Field Ionization and Field Desorption Mass Spectrometry, Pergamon, Oxford, 1977.
13 W.W. Hunt, R.E. Huffman and K.E. McGee, Rev. Sci. Instr. 35 (1964) 82.
14 B.T. Chait and F.H. Field, Submitted for publication to J. Am. Chem. Soc.
15 P.J. Robinson and K.A. Holbrook, Unimolecular Reactions, Wiley, London,1972.